

13. THE FORMATION DENSITY LOG

13.1 Introduction

The *formation density log* measures the bulk density of the formation. Its main use is to derive a value for the total porosity of the formation. It is also useful in the detection of gas-bearing formations and in the recognition of evaporites.

The formation density tools are induced radiation tools. They bombard the formation with radiation and measure how much radiation returns to a sensor.

13.2 Theory

The tool consists of:

- **A radioactive source.** This is usually caesium-137 or cobalt-60, and emits gamma rays of medium energy (in the range 0.2 – 2 MeV). For example, caesium-137 emits gamma rays with an energy of 0.662 MeV.
- **A short range detector.** This detector is very similar to the detectors used in the natural gamma ray tools, and is placed 7 inches from the source.
- **A long range detector.** This detector is identical to the short range detector, and is placed 16 inches from the source.

The gamma rays enter the formation and undergo Compton scattering by interaction with the electrons in the atoms composing the formation, as described in Section 9.3. Compton scattering reduces the energy of the gamma rays in a step-wise manner, and scatters the gamma rays in all directions. When the energy of the gamma rays is less than 0.5 MeV they may undergo photo-electric absorption by interaction with the atomic electrons. The flux of gamma rays that reach each of the two detectors is therefore attenuated by the formation, and the amount of attenuation is dependent upon the density of electrons in the formation.

- A formation with a high bulk density, has a high number density of electrons. It attenuates the gamma rays significantly, and hence a low gamma ray count rate is recorded at the sensors.
- A formation with a low bulk density, has a low number density of electrons. It attenuates the gamma rays less than a high density formation, and hence a higher gamma ray count rate is recorded at the sensors.

The density of electrons in a formation is described by a parameter called the *electron number density*, n_e . For a pure substance, number density is directly related to bulk density, and we can derive the relationship in the following way.

- The number of atoms in one mole of a material is defined as equal to Avogadro's number N ($N \approx 6.02 \times 10^{23}$).
- The number of electrons in a mole of a material is therefore equal to NZ , where Z is the atomic number (i.e., the number of protons, and therefore electrons per atom).

- Since the atomic mass number A is the weight of one mole of a substance, the number of electrons per gram is equal to NZ/A .
- However, we want the number of electrons per unit volume, and we can obtain this from the number of electrons per gram by multiplying by the bulk density of the substance, r_b . Hence, the electron number density is

$$n_e = \frac{N Z}{A} r_b \quad (13.1)$$

where: n_e = the number density of electrons in the substance (electrons/cm³)
 N = Avagadro's number ($\approx 6.02 \times 10^{23}$)
 Z = Atomic number (no units)
 A = Atomic weight (g/mole)
 r_b = the bulk density of the material (g/cm³).

Thus, the gamma count rate depends upon the electron number density, which is related to the bulk density of a substance by Eq. (13.1). The bulk density of a rock depends upon the solid minerals of which it is composed, its porosity, and the density of the fluids filling that porosity. Hence, the formation density tool is useful in the determination of porosity, the detection of low density fluids (gasses) in the pores, and as an aid in lithological identification.

13.3 Operation

A radiation emitter and one detector are all that is necessary for a simple measurement. The early tools had only one detector, which was pressed against the borehole wall by a spring-loaded arm. Unfortunately, this type of tool was extremely inaccurate because it was unable to compensate for mudcake of varying thicknesses and densities through which the gamma rays have to pass if a measurement of the true formation is to be achieved.

All the newer tools have two detectors to help compensate for the mudcake problem. The method of compensation is described in subsequent sections. The newer two detector tools are called compensated formation density logs, an example of which is Schlumberger's FDC (formation density compensated) tool.

Compensated formation density tools have one focussed (collimated) radiation source, one short spacing detector at 7 inches from the source, and one long spacing detector 16 inches from the source (Fig. 13.1). The source and both detectors are heavily shielded (collimated) to ensure that the radiation only goes into the mudcake and formation, and that detected gamma rays only come from the mudcake or formation. The leading edge of the shield is fashioned into a plough which removes part of the mudcake as the tool is pulled up the well. The tool is pressed against one side of the borehole using a servo-operated arm with a force of 800 pounds force. Under this pressure and the pulling power of the wireline winch the plough can make a deep impression in the mudcake. The large eccentric force also means that there is much wear of the surface of the tool that is pressed against the borehole wall. The heavy shielding also doubles as a skid and a wear plate that protects the source and detectors and can be replaced easily and cheaply when worn down.

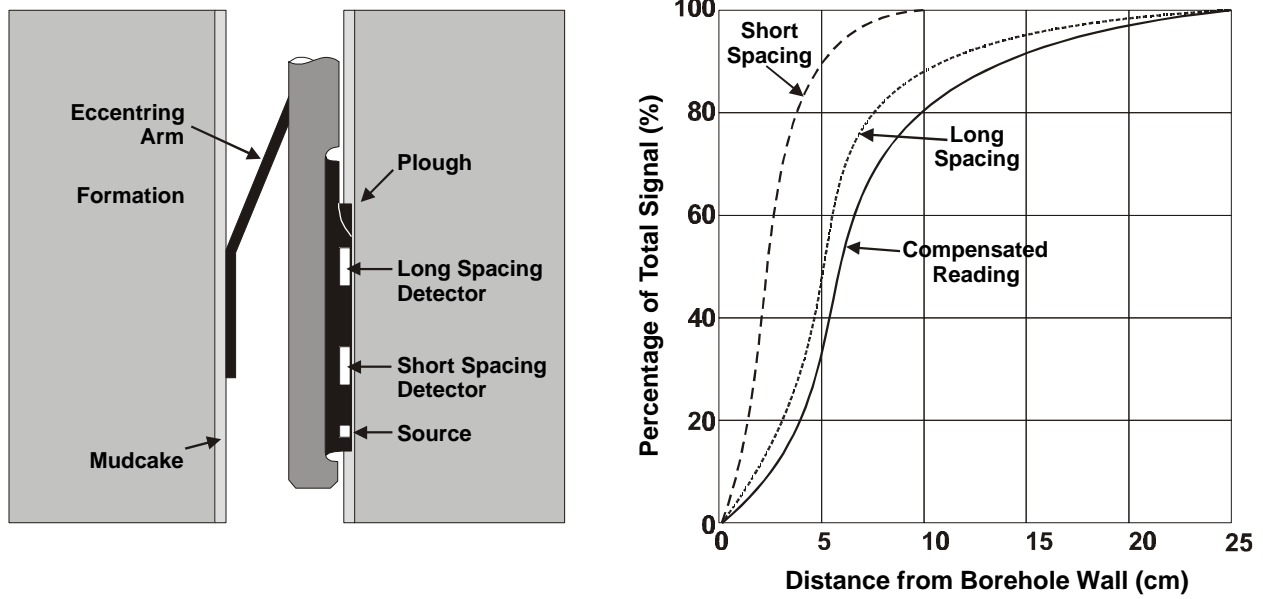


Figure 13.1 Schematic diagram of a formation density tool.

The operation of this tool depends upon the detection of gamma rays that have been supplied to the formation by the source on the tool and have undergone scattering. Clearly the natural gamma rays from the formation confuses the measurement. A background gamma ray count is therefore carried out so that the gamma rays coming from the formation can be removed from the measurement.

Note in Fig. 13.1 that for the short spacing detector over 80% of its signal comes from within 5 cm of the borehole wall, which is commonly mainly mudcake. About 80% of the long spacing signal comes from within 10 cm of the borehole wall. Therefore the tool has a shallow depth of investigation. We wish to remove the mudcake signal from the measurement, and the procedure to do this is described in Section 13.4. When the mudcake compensation has been carried out, one can see from Fig. 13.1 that the depth of investigation has been improved, and less signal comes from the first 5 cm region.

13.4 Mudcake Compensation

Gamma rays detected by the short spacing detector have penetrated only a short way into the mudcake and formation before being scattered back to the detector. Readings from the short spacing detector are therefore a measure of attenuation in the near-borehole region (i.e., mudcake and very shallow in the formation). By comparison, gamma rays detected by the long spacing detector have penetrated through the mudcake and deeper into the formation before being scattered back to the detector. Readings from the long spacing detector are therefore a measure of attenuation in the formation that has been perturbed by the gamma rays having to pass through the mudcake twice.

The compensation scheme described below effectively takes the effect of the near-borehole region (short spaced detector) away from the formation plus near-borehole region (long spacing detector). This sounds easy but is not straightforward.

For any given borehole and tool geometry there are eight independent parameters that affect the reading of the tool. These are:

- Z_b = the mean atomic number of the formation
- A_b = the mean atomic weight of the formation
- r_b = the bulk density of the formation
- Z_{mc} = the mean atomic number of the mudcake
- A_{mc} = the mean atomic weight of the mudcake
- r_{mc} = the bulk density of the mudcake
- h_{mc} = the thickness of the mudcake

The influence of changing Z_b , A_b and A_{mc} are small, and so these parameters can be considered to be constant. Unfortunately we cannot assume that Z_{mc} is constant as the drilling mud (and hence mudcake) may or may not contain barite in very significant quantities.

The number of variable parameters is reduced to three by the incorporation of r_{mc} and Z_{mc} into a single parameter, the effective mudcake density r_{mc}^* , which combines the influences of both r_{mc} and Z_{mc} . The remaining three parameters are r_b , r_{mc}^* and h_{mc} .

These three parameters are represented as a function of the readings from the short and long spacing detectors by a single and rather clever graph. The y-axis (ordinate) of the graph is the reading from the long spacing detector, and the x-axis (abscissa) of the graph is the reading from the short spacing detector. Points plot on this graph in different ways depending upon the various values of r_b , r_{mc}^* and h_{mc} .

Imagine that there is no mudcake. The short spaced detector will make a reading of gamma count rate that is dependent upon the short path between the source and the detector through the formation. The long spaced detector will also make a reading, which will be lower because of the greater distance of this detector from the source.

The readings from the long and short spaced detectors will fall on a straight line (Fig. 13.2). The higher the readings, the less dense the formation and *vice versa*. So we can calibrate the straight line to be read in terms of the bulk density of the formation. This line is called the *spine* of the plot.

Now imagine that a mud of variable thickness and $r_{mc}^*=1.5 \text{ g/cm}^3$ is present on the borehole wall, and the formation density is 2.5 g/cm^3 . If the mudcake does not exist the detector values plot at point A in Fig. 13.3 as expected. If the mudcake thickness increases, the short spaced detector sees more of the less dense mudcake, and so gives a higher count rate. The long spaced detector also give a higher count rate due to the lower density mudcake that is present, but the increase is initially marginal because the long spaced detector is sensitive to a region which the mudcake only forms a small part. The result is the curve shown in Fig. 13.3. Note that this curve leaves the spine at 2.5 g/cm^3 , when $h_{mc}=0$, forms an arc to the right of the spine, and rejoins the spine at 1.5 g/cm^3 as $h_{mc}\rightarrow\infty$. The rejoining represents the state where the thickness of the mudcake is greater than the depth of investigation of the tool, so that both the long and short spaced detectors read only mud. The curved part of the graph therefore represents the complete range of mudcake thicknesses.

If the effective mudcake density remains at 1.5 g/cm^3 , but the formation density changes, the bottom point where the curved part of the line joins the spine slides up and down the spine, as shown in Fig. 13.4 for formation densities of 2.0, 2.5 and 3.0 g/cm^3 . Each of the curved lines represents a different formation density, leaving the spine at the formation density value for $h_{mc}=0$, and rejoining the spine together at the effective mudcake density of 1.5 g/cm^3 .

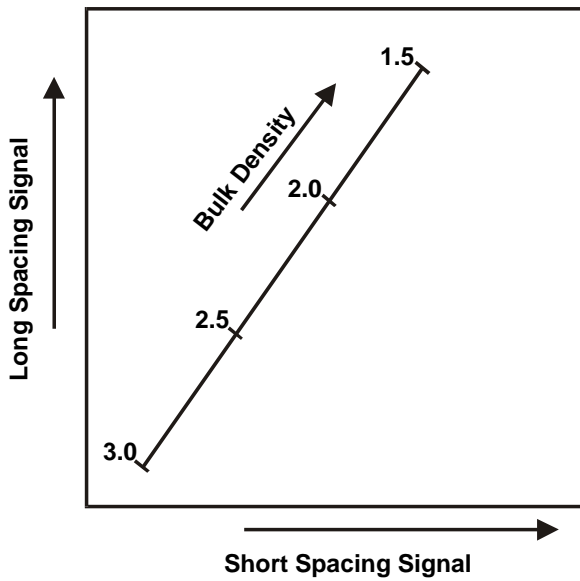


Figure 13.2 Formation density tool mudcake correction plot (spine and ribs) with no mudcake present.

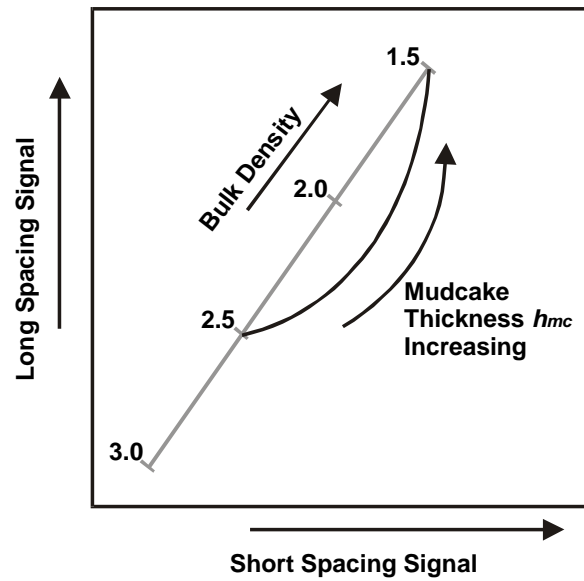


Figure 13.3 Formation density tool mudcake correction plot (spine and ribs) with $r_b=2.5 \text{ g/cm}^3$, $r_{mc}^*=1.5 \text{ g/cm}^3$, and variable thickness mudcake.

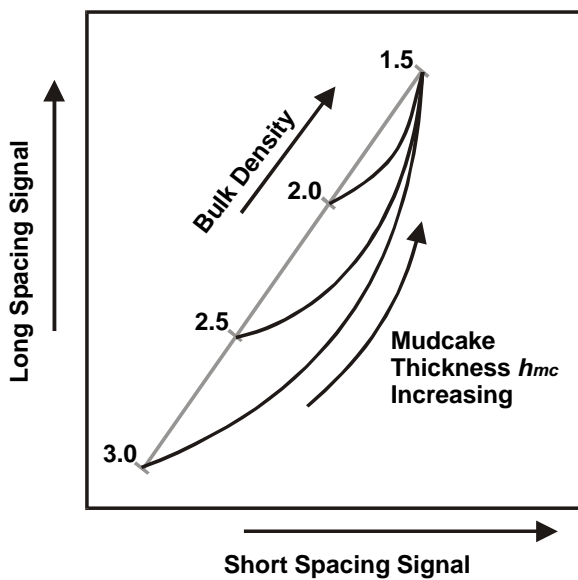


Figure 13.4 Formation density tool mudcake correction plot (spine and ribs) with $r_b=2.0, 2.5$ and 3.0 g/cm^3 , $r_{mc}^*=1.5 \text{ g/cm}^3$, and variable thickness mudcake.

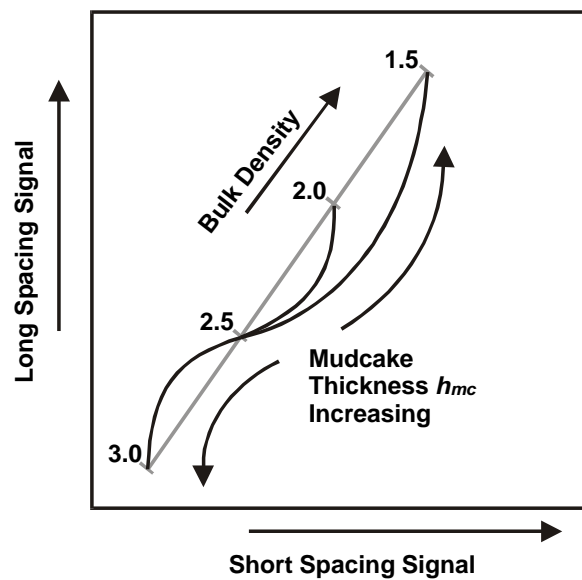


Figure 13.5 Formation density tool mudcake correction plot (spine and ribs) with $r_b=2.5 \text{ g/cm}^3$, $r_{mc}^*=1.5, 2.0$ and 3.0 g/cm^3 , and variable thickness mudcake.

If the formation density remains fixed at 2.5 g/cm^3 the point where the curved portion of the line leaves the spine is fixed at 2.5 g/cm^3 . Now, if the effective mudcake density changes, the point where the curved part of the line rejoins the spine slides up and down the spine, as shown in Fig. 13.5 for effective mudcake densities of 1.5, 2.0 and 3.0 g/cm^3 . Each of the curved lines represents a different effective mudcake density, leaving the spine at the formation density value of 2.5 g/cm^3 for $h_{mc}=0$, and rejoining the spine together at the relevant effective mudcake density, which may be above or below the formation density on the spine.

Note that if the effective mudcake density is the same as the formation density, the curved portion of the line does not exist, and the tool interprets the mudcake as formation.

In practice, only portions of the curved lines are relevant to wellbore conditions. Over the practical range, the combination of the curves and the spine is reminiscent of a rib-cage. This type of plot is therefore called a *spine and ribs plot*.

Figure 13.6 shows a spine and ribs plot for the formation density tool during a well controlled laboratory study of the tool. Note that the data on each rib is practically independent of effective mudcake density and composition, and that as mudcake becomes thicker, the data points lie further up or down the rib from the spine as expected.

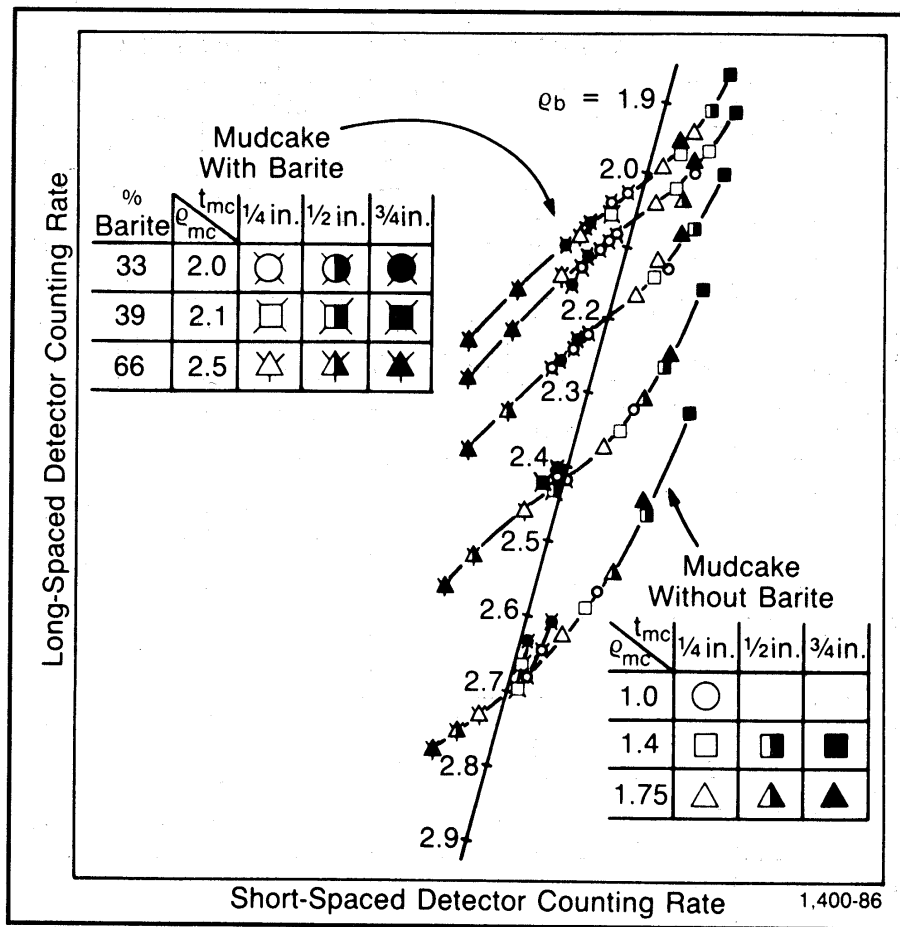


Figure 13.6 Formation density tool mudcake correction plot (spine and ribs) from laboratory derived calibration data.

The spine and ribs plot therefore has the advantages that (i) the variation in effective mudcake density and mudcake thickness can be described by a single parameter (the distance up a given rib), (ii) for each formation density, all ribs leaving one side of the graph coincide on the spine at a single point (the effective mudcake density), and (iii) knowing the spine and ribs plot for a given tool, the long and short detector readings can be used to obtain the corrected value of formation density without explicit measurement of either the effective mudcake density or the mudcake thickness. The correction procedure is automated in modern tools.

13.5 Calibration

The direct relationship between electron number density and bulk density indicates that no calibration is necessary. However, hydrogen is anomalous, and its presence perturbs the direct relationship. For this reason the formation density tools are calibrated. The primary calibrations are made by inserting the tool into a block of pure limestone saturated with fresh water of accurately known density. Secondary (check) calibrations are made in the wireline tool workshop by inserting the tool into large blocks of aluminium, sulphur and magnesium of known density. Sleeves of varying thickness are put around the tool to simulate mudcake thickness to check the operation of the automatic mudcake compensation process. A portable radiation source is used at the wellsite to check the responses of the two detectors before and after the tool has been run.

The relationship between electron number density and the bulk density is given by Eq. (13.1). Note that there is a linear relationship between the electron number density and the bulk density, and the remaining parameters in the equation are either constant for a given element (A and Z), or universally constant (N). Table 13.1 shows the values of A , Z , Z/A and $2Z/A$ for common elements in the crust.

Table 13.1 Atomic number and mass data for common elements in the crust.

Element	Z	A	Z/A	$2Z/A$
H	1	1.0079	0.99215	1.9843
C	6	12.0111	0.4995	0.999
O	8	15.9994	0.5	1.000
Na	11	22.9898	0.47845	0.9569
Mg	12	24.3120	0.4936	0.9872
Al	13	26.9815	0.4818	0.9636
Si	14	28.086	0.49845	0.9969
S	16	32.064	0.499	0.9980
Cl	17	35.453	0.4795	0.9590
K	19	39.102	0.4859	0.9718
Ca	20	40.080	0.499	0.9980

Note that Z/A is close to 0.5 for all elements except hydrogen, which is almost unity.

We define a new parameter called the effective number density r_e , where $r_e = 2 n_e/N$. Hence, Eq. (13.1) becomes

$$r_e = \frac{2Z}{A} r_b \tag{13.2}$$

For rocks that are composed of more than one element, Eq. (13.2) is valid providing that Z is the mean atomic number and A is the mean atomic mass.

For most elements, the constant term is almost unity giving a one to one calibration. For hydrogen the equation breaks down. We can examine the effect of the hydrogen on Eq. (13.2) by carrying out a calibration of the tool in limestone saturated with fresh water, where its density is accurately known. This calibration provides the relationship

$$r_a = 1.07 \times r_e - 0.188 \tag{13.3}$$

where r_a is the apparent density (that read by the tool). For water-filled sandstones, limestones and dolomites the tool reading is almost identical to the actual bulk density. Table 13.2 compares the apparent density read by the tool against the actual bulk density.

Table 13.2 Comparison of apparent density measured by the formation density tool with the actual bulk density for common mineralogies and fluids.

Compound	Composition	Actual Bulk Density, r_b	$2Z/A$	Effective Electron Density, r_e	Apparent Bulk Density, r_a
Quartz	SiO ₂	2.654	0.9985	2.650	2.648
Calcite	CaCO ₃	2.710	0.9991	2.708	2.710
Dolomite	CaCO ₃ .MgCO ₃	2.870	0.9977	2.863	2.876
Anhydrite	CaSO ₄	2.960	0.9990	2.957	2.977
Sylvite	KCL	1.984	0.9657	1.916	1.863
Halite	NaCl	2.165	0.9581	2.074	2.032
Gypsum	CaSO ₄ .2H ₂ O	2.320	1.0222	2.372	2.351
Anthracite (low)		1.400	1.030	1.442	1.355
Anthracite (high)		1.800	1.030	1.852	1.796
Coal (Bituminous)		1.200	1.060	1.272	1.173
Coal		1.500	1.060	1.590	1.514
Pure Water	H ₂ O	1.000	1.1101	1.110	1.000
Salt Water	200,000 ppm NaCl	1.146	1.0797	1.237	1.135
Oil	(CH ₂) _n	0.850	1.1407	0.970	0.850
Methane	CH ₄	r_m	1.247	1.247 r_m	1.335 r_m - 0.188
Gas	C _{1.1} H _{4.2}	r_g	1.238	1.238 r_g	1.325 r_g - 0.188

The density in some formations such as anhydrite, sylvite and halite must be corrected, as do readings in gas-bearing formations. Figure 13.7 shows the corrections that need to be made.

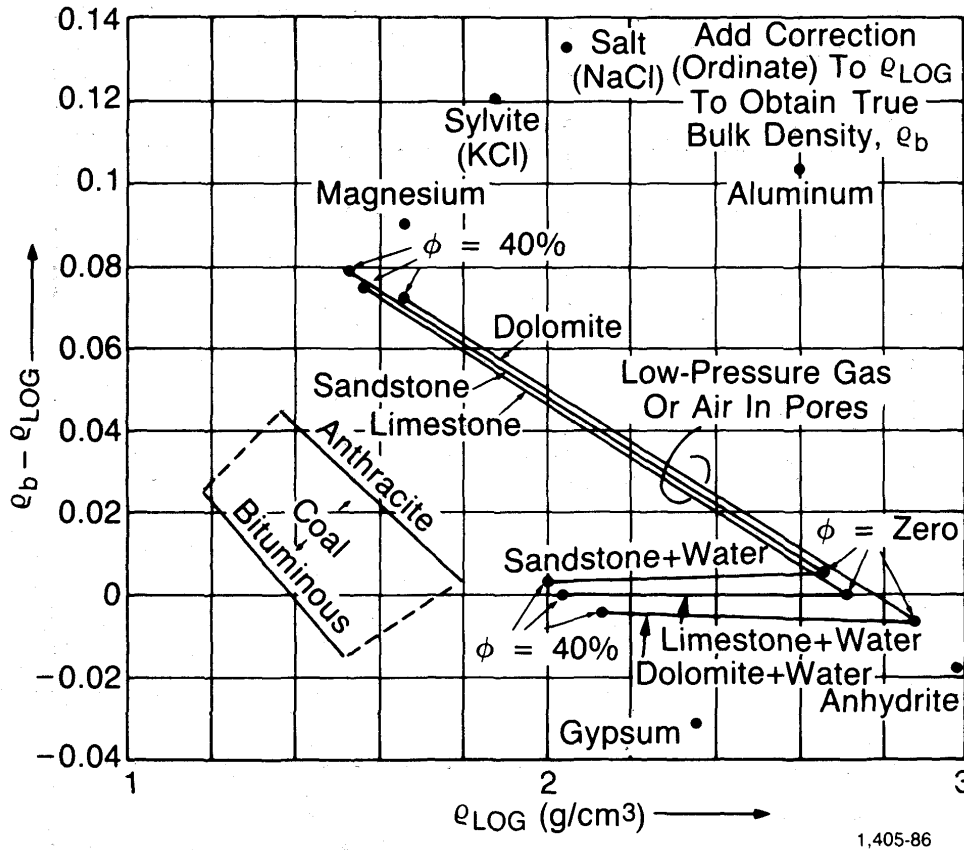


Figure 13.7 Formation density tool mineral correction plot.

Corrections also need to be made if the borehole is larger than 10 inches in diameter. The correction curve for one tool is given in Fig. 13.8.

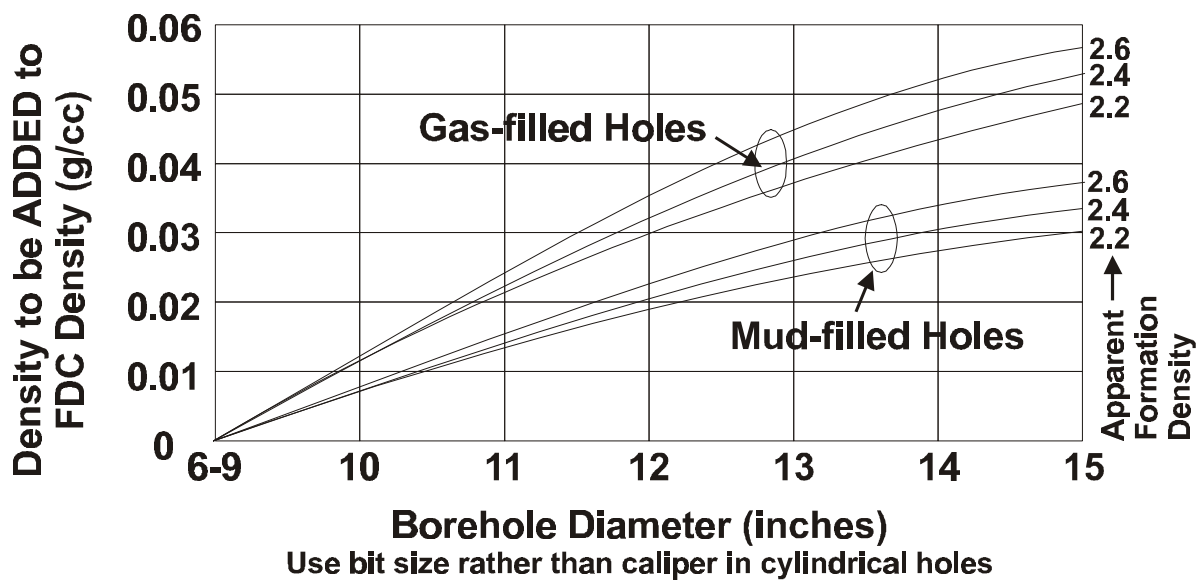


Figure 13.8 Formation density tool hole diameter correction plot.

13.6 Log Presentation

The formation density log is recorded in tracks 2 and 3 of the standard API log presentation on a linear scale. The scale is in g/cm^3 , and usually spans 1.95 to 2.95 g/cm^3 as this is the normal range for rocks (Fig. 13.9).

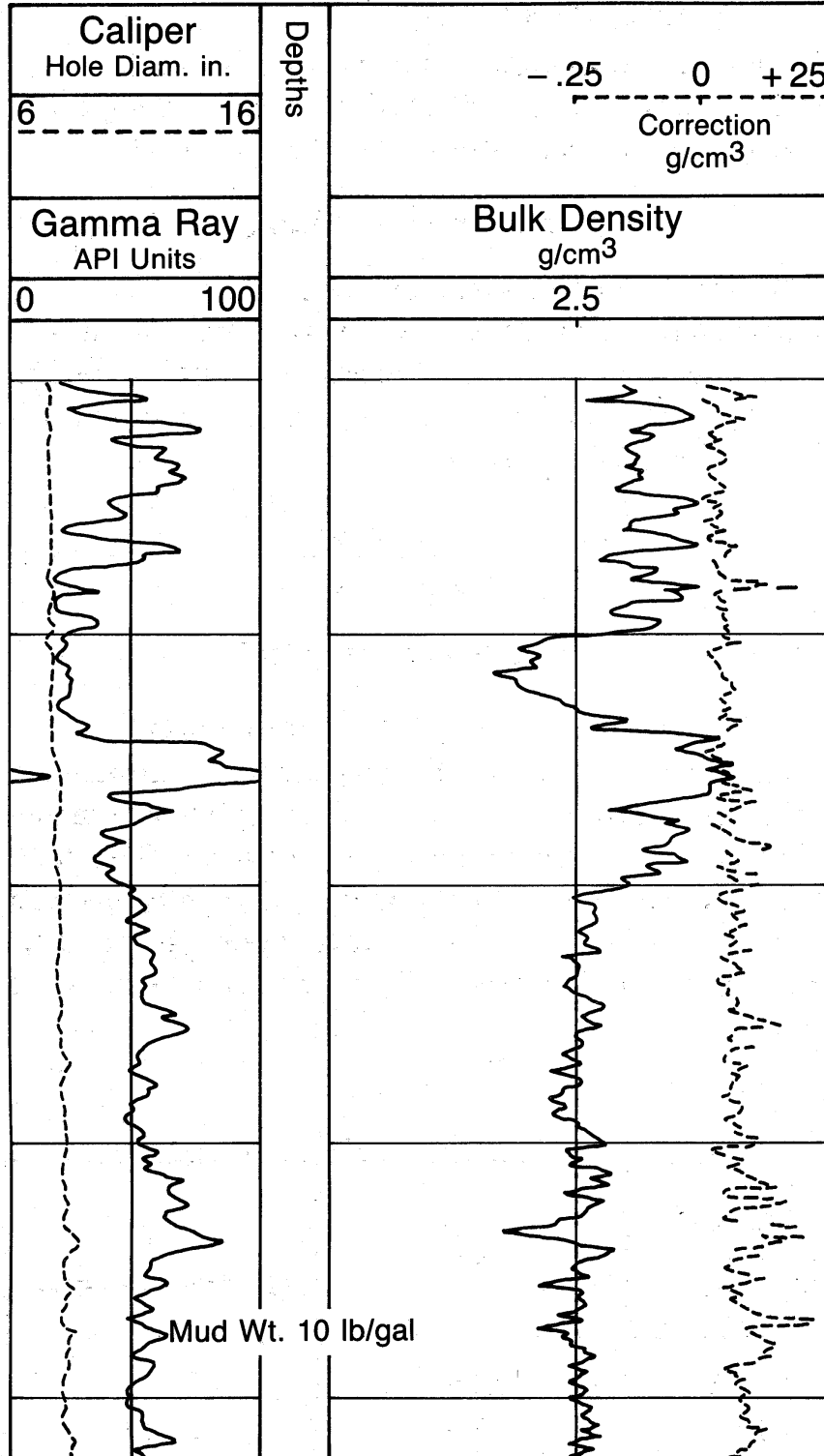


Figure 13.9 Formation density tool log presentation.

The automatic compensation (correction) for mudcake is often shown in either track 2 or track 3 on a linear scale. This curve is included as a quality control curve. If the correction curve is greater than $\pm 0.15 \text{ g/cm}^3$, the data in the main curve will not be very reliable.

As the formation density tool is a log that is commonly used to calculate porosity, a pseudo-porosity that has been calculated from the density data may be shown together with the bulk density curve and correction curve. This is a pseudo-porosity curve because it will assume a matrix and fluid density to be constant throughout the logged interval. Matrix densities of 2.65 g/cm^3 (for quartz) and fluid densities of 1.1 g/cm^3 (for salt water) are often used.

A wireline tension curve is often also included in the record, because the formation density tool is prone to getting stuck in holes as a result of its ploughing in sticky mudcake.

The formation density tool is most often run in combination with (i) a gamma ray log, for depth matching, (ii) a caliper log, for borehole quality control, and (iii) a neutron log, because the interpretation of the formation density tool together with the results from the neutron log provide one of the two best lithological assessment techniques for a reservoir.

13.7 Depth of Investigation

The depth of investigation of the tool is very shallow. For Schlumberger's FDC tool 90% of the response comes from the first 13 cm (5 inches) from the borehole wall for a 35% porosity sandstone (which has low density compared with most reservoir rocks). In higher density rocks the depth of investigation is even less, and a value of about 10 cm (4 inches) can be taken as an average value for reservoir rocks. Figure 13.1 shows the percentage of the signal that comes from different depths into the formation.

The shallow depth of investigation of the tool makes it sensitive to borehole quality, and it is therefore necessary to interpret the formation density log together with the caliper log to ensure that the measured values is not an artifact of bad hole quality.

The shallow depth of investigation also implies that in porous and permeable formations, where its main use lies, it only measures the invaded zone. This should be taken into consideration when deciding on a fluid density (mud filtrate density) to use for porosity calculations. The fact that the tool only measures the invaded zone in porous formations makes the tool little use for distinguishing between formation oil and formation water. However, gas may still be detected because (i) the greater difference in density between gas and oil or water, and (ii) the fact that mud filtrate invasion into gas-bearing zones is never complete, and always leaves a significant amount of gas behind in the invaded zone.

13.8 Logging Speed

The typical logging speed for the tool is 1300 ft/hr (400 m/hr), although it is occasionally run at lower speeds to increase the vertical resolution. The log quality is not as effected by logging speed as the natural gamma ray logs because much higher count rates are obtained with the radioactive source on the tool.

13.9 Vertical Resolution

The vertical resolution at the typical logging speed (1300 ft/hr) is good (about 26 cm, 10 inches), which is defined by the distance between the two detectors. The measurement point is taken to be half way between the two detectors. Beds can be resolved down to about 60 cm (2 ft) with the density tool reading the true density value of the bed. Even better resolutions are possible with slower logging speeds. Partial reaction of the logging tool to very thin beds of anomalously high or low density is sometimes encountered. For example, thin (5 – 10 cm thick) layers of calcareous nodules.

The high vertical resolution means that the log is useful for defining formation boundaries.

13.10 Borehole Quality

The log is run eccentric in the borehole, and therefore is prone to caving and rough borehole walls where the detectors or the source may not be pressed against the borehole wall. In this case the readings will be erroneous due to radiation leakage along the borehole between the detectors and bad measurement geometry. The sensitivity to bad hole quality is exacerbated by the shallow depth of investigation that the tool has. The formation density log should, therefore be run with a caliper tool, and the caliper reading should be used to judge the likely quality of the formation density log data.

13.11 Mud Type

Drilling muds with high density or that absorb gamma rays efficiently, such as barite filled muds, will effect the detector readings. However, the effect of these muds is compensated for automatically by the spine and ribs correction.

13.12 Uses of the Formation Density Log

The main use of the formation density log is to determine porosity. It has numerous other uses, the main ones being the recognition of gas-bearing zones, and the identification of minerals (particularly evaporites). The combination of formation density log data with neutron log data gives one of the best ways of identifying lithologies in a borehole. This will be described in Chapter 15.

13.12.1 Determination of Porosity

The porosity f of a formation can be obtained from the bulk density if the mean density of the rock matrix and that of the fluids it contains are known.

The bulk density r_b of a formation can be written as a linear contribution of the density of the rock matrix r_{ma} and the fluid density r_f , with each present in proportions $(1 - f)$ and f , respectively :

$$r_b = (1 - f)r_{ma} + f r_f \quad (13.4)$$

When solved for porosity, we get

$$f = \frac{r_{ma} - r_b}{r_{ma} - r_f} \tag{13.5}$$

where: r_b = the bulk density of the formation
 r_{ma} = the density of the rock matrix
 r_f = the density of the fluids occupying the porosity
 f = the porosity of the rock.

The fluid densities are usually available from RFT sampling, but values of 1.0 g/cm³ for fresh water and 1.1 g/cm³ for salt water are often used. Remember that the tool measures the invaded zone, so the relevant fluid is the mud filtrate in most circumstances. If available, the fluid densities should be corrected to borehole temperature conditions. If the formation is hydrocarbon-bearing the fluid density can be calculated by

$$r_f = r_{mf} S_{XO} + r_{hc} (1 - S_{XO}) \tag{13.6}$$

where: S_{XO} = the saturation of the mud filtrate in the invaded zone
 r_{mf} = the density of the mud filtrate
 r_{hc} = the density of the hydrocarbon
 r_f = the fluid density.

The value of the matrix density taken depends upon the lithology of the interval under question. For sandstones, the density of quartz is 2.65 g/cm³, and for limestones, the density of calcite is 2.71 g/cm³. Clay minerals have varied grain densities. Often core data is used to provide accurate matrix densities for particular intervals.

Table 13.3 gives the matrix densities of some common minerals.

Table 13.3 Grain (matrix) densities of some common rock forming minerals.

Mineral	Grain Density (g/cm ³)	Mineral	Grain Density (g/cm ³)
Quartz	2.65	Halite*	2.16
Calcite	2.71	Gypsum*	2.30
Dolomite	2.87	Anhydrite*	2.96
Biotite	2.90	Carnalite*	1.61
Chlorite	2.80	Sylvite*	1.99
Illite	2.66	Polyhalite*	2.78
Kaolinite	2.594	Glauconite	2.30
Muscovite	2.83	Kainite	2.13

*Evaporites

Care must be taken within some lithological intervals because the composition of the matrix may change. For example, the grain density for a clean sandstone is that of quartz (2.65 g/cm³). However, if there is a variable amount of biotite present mixed in with the sand, the bulk density of the rock can rise to 2.84 g/cm³ because biotite has a density of 2.9 g/cm³. This scenario is encountered in some North Sea reservoirs. Analysis of Eq. (13.3) shows that an error of 0.01 g/cm³ in the matrix density gives an error of 0.5% in the calculated porosity, which gives an error of almost 10% if a matrix

density of 2.65 g/cm^3 is assumed for a sand that has an actual density of 2.84 g/cm^3 due to additional biotite.

The Effect of Fluid Density. The porosity may also be in error if the fluid density is misjudged. The fluid existing in the zone of the rock measured by the formation density tool is usually mud filtrate. The density of these fresh and salt waters is approximately 1.0 g/cm^3 and 1.1 g/cm^3 , respectively. However, these vary with temperature and composition, so accurate values for the actual reservoir formation water at the relevant reservoir temperatures should be used wherever possible. Such data can be obtained from samples of reservoir fluid from RFT analysis, or from the analysis of mud filtrate, bearing in mind that the tool measures the invaded zone, so the relevant fluid density to use in the porosity calculations is most often the mud filtrate density. Mud filtrate densities are now corrected automatically for temperature and pressure in most petrophysical software. However, the correction used to be carried out with the aid of a nomogram.

The Effect of Gas. If gas is present in the formation, porosities can be overestimated. The density of gasses is very low (approximately 0.0001 g/cm^3) compared to aqueous fluids. If the formation is gas-bearing a significant amount of gas is always left in the invaded zone. This gas will reduce the mean fluid density of the invaded zone, and will cause overestimations of the porosity if a fluid density of 1.0 or 1.1 g/cm^3 is used as shown in Fig. 13.10.

The Effect of Oil. The density of oil (approximately 0.7 g/cm^3) is less than that of aqueous fluids. However the presence of oil-bearing formations rarely causes problems in porosity calculation because both the oil and water in the invaded zone, which the tool measures, is replaced by mud filtrate.

The Effect of Shale. The density of shales varies greatly, and if present as a proportion of a lithology (such as a shaly sandstone or shaly limestone) can make the derivation of a reliable porosity inaccurate. If we have zones of clean lithology and zones of shale with a shaly sandstone in between (or a full fining-up or coarsening-up sequence), we can use the bulk densities in the shale and clean sandstone together with V_{sh} to obtain a corrected density for the shaly sandstone at any given depth.

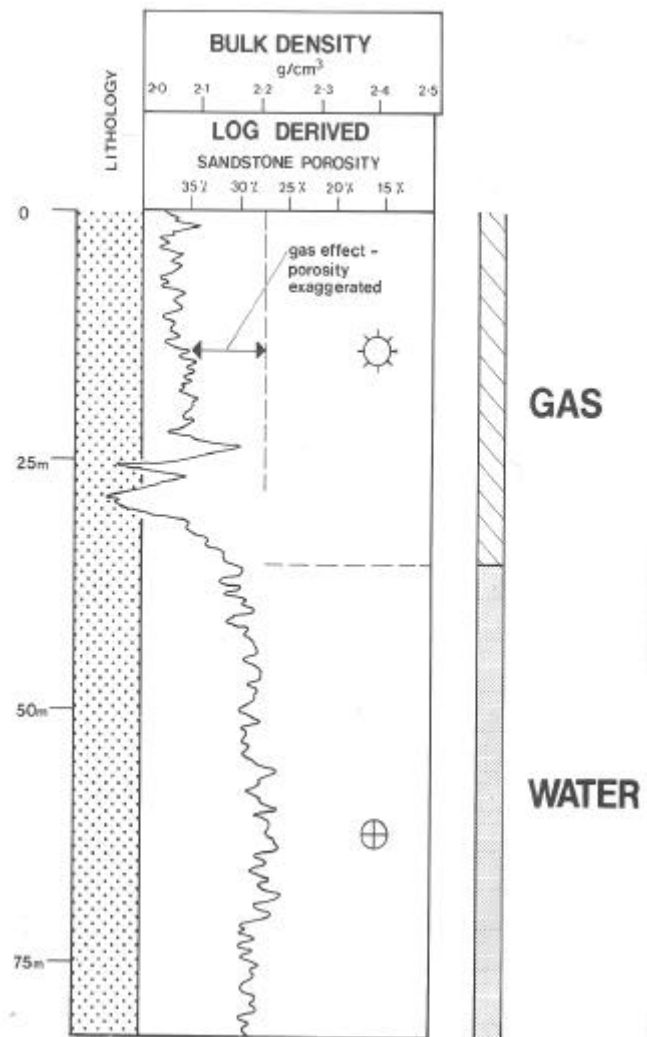


Figure 13.10 The effect of gas on the formation density log.

This corrected value of density may then be used in Eq. (13.5) to obtain a porosity which takes account of the shaliness of the sandstone (or limestone). The corrected bulk density of the shaly lithology is given by

$$(r_b)_{corr} = (r_b)_{clean} (1 - V_{sh}) + (r_b)_{shale} V_{sh} \tag{13.7}$$

Calibration with Core Porosities. The most accurate porosity determinations are obtained from laboratory measurements on cores. If there is a database of core porosities for a given well, it is often advantageous to plot the core porosity against the formation density log derived porosity or (better) the bulk density from the formation density log. The first type of plot should show the points lying on a 1:1 straight line. The second type of plot also gives a straight line with a negative gradient (Fig. 13.11). Non-linearity in the second type of plot indicates problems with the formation density log, while the first type of plot can be used to indicate that there is a better matrix or fluid density to use to transform the measured bulk density data to reliable porosity values.

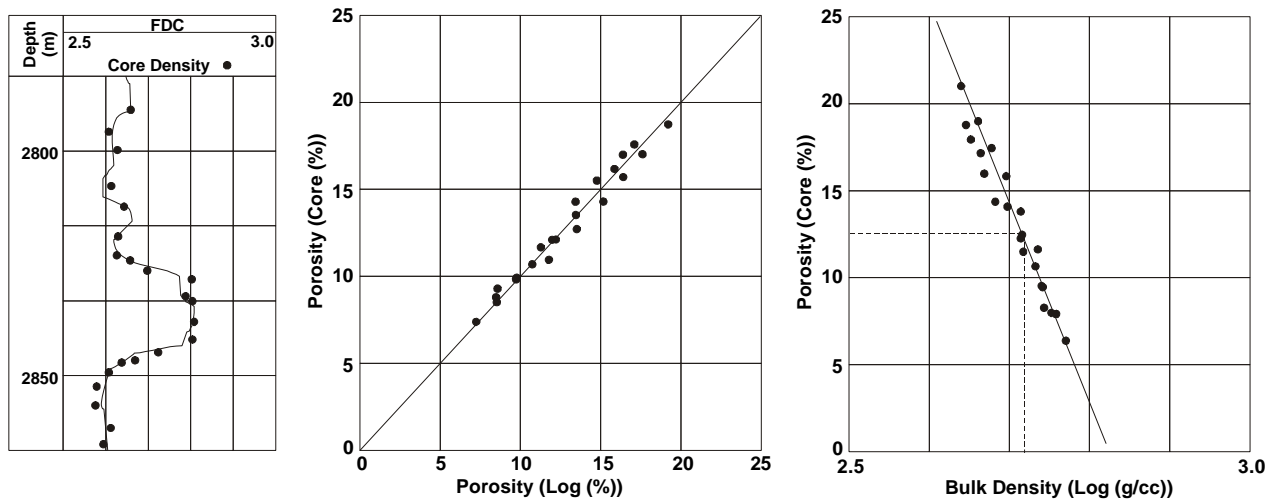


Figure 13.11 Calibration of the formation density tool against core porosities.

13.12.2 Acoustic Impedance

Density from the formation density log is often combined with acoustic velocity from the sonic log to calculate acoustic impedance down a well. The acoustic impedance can be used to create synthetic seismograms to help the interpretation of seismic data.

13.12.3 Identification of Lithology

When used alone, the density log is not a good tool for identifying most lithologies. This is because most rocks have a wide range of densities resulting from their varied mineralogical compositions and their variable porosities. For example, shales have bulk densities ranging from 1.8 to 2.8 g/cm³ and have variable clay mineral densities. Sandstones, limestones and dolomites all have bulk density

ranges that overlap each other and that of shales (Fig. 13.12). However, when used with the neutron log, the combination is a very good lithological determination method (as described in Chapter 15).

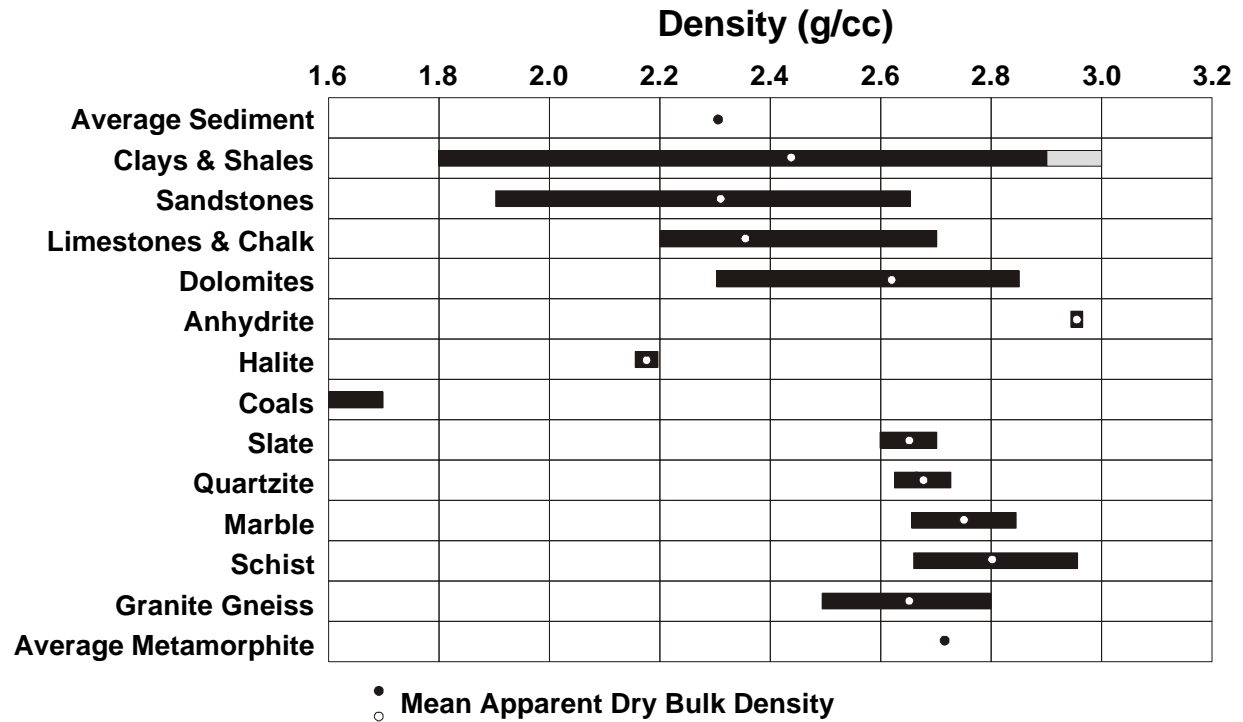


Figure 13.12 Density ranges of common lithologies.

13.12.4 Identification of Evaporites

Evaporites are often found in a very pure state, and have clearly defined densities. If evaporites are recognized within a log sequence, their type may be determined directly and unambiguously from the formation density log bulk density value. Table 13.1 gives data for some commoner evaporites.

13.12.5 Shale Compaction, Age, and Unconformities

Shale undergoes progressive compaction and increasing density with depth of burial and age. Occasionally, if the formation density data is plotted on a sufficiently small depth scale, the compaction trend may be noted by a steady but small rate of increase of density with depth (Fig. 13.13). It is a rule of thumb that the more compact shales are older (although this is not always the case).

If, within a given shale interval, there is a sudden change of density, the most likely explanation is that the formations above and below the change have been deposited in a completely different environment. The change is therefore an indication of a possible unconformity (Fig. 13.14).

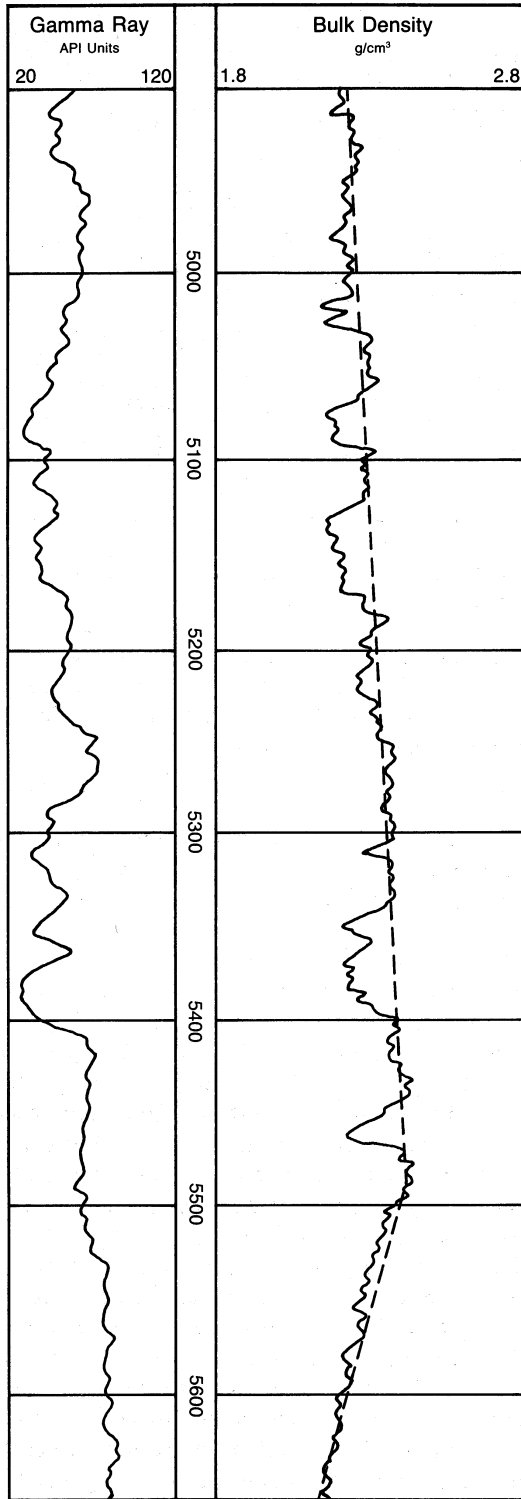


Figure 13.13 Recognition of shale compaction and overpressure in shale sequences using the formation density log.

13.12.6 Overpressure

Fluid overpressure works against any compaction trend caused by the overburden pressure. Hence, it is likely that overpressured zones will retain a greater porosity than normally pressured zones. If a normal compaction or no compaction is observed in a shale over some depth interval, and below it the bulk density begins to decrease (or the derived porosity begins to increase) without change in lithology, it is likely that one has entered a zone of overpressured fluids. In this zone the overpressured fluids keep the porosity open, stopping any compaction trend and reversing it (Fig. 13.13).

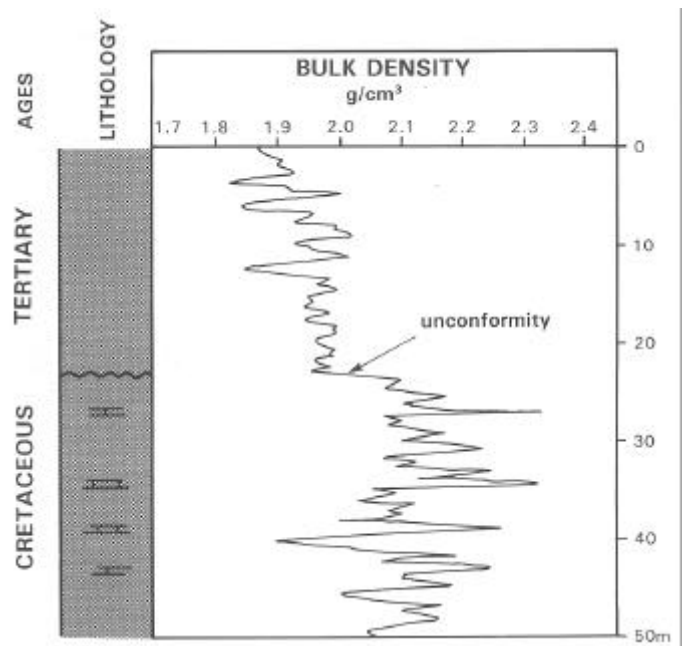


Figure 13.14 Recognition of unconformities in shale sequences using the formation density log.

13.12.7 *Recognition of Accessory Mineralogies*

Thin bands of anomalously high or low density within a single lithology, or a change in the character of the density log within a single lithology indicates that there are additional mineral present. Examples of this may be:

Thin bands of siderite in shales	Thin density peaks
Thin bands of carbonate nodules in shales or sandstones	Thin density peaks
Thin bands of carbonate in shales or sandstones	Thin density peaks
Thin bands of heavy or radioactive placer minerals	Thin density peaks
Dispersed micas in sandstones	Increased densities in affected zone

Mineralogies and lithologies that lower the density locally if present in thin bands include lignite, coal, anthracite or increased organic matter in a shale.

Mineralogies and lithologies that increase the density locally if present in thin bands include pyrite, siderite, basalt and gneiss.

13.12.8 *Fracture Recognition*

The density tool records the bulk density of the formation. The porosity derived from this will include all pores and fractures whether they are connected or not.

The sonic tool can also be used to measure the porosity of the formation. However, the sonic tool is not sensitive to fracture porosity.

Hence, the difference between the porosities derived from these two measurements can be used as an indicator of the extent of fracturing in a reservoir interval.

13.12.9 *Organic Content of Source Rocks*

The presence of organic matter can reduce the density of shales by up to 0.5 g/cm^3 . It is possible to calculate the total organic carbon (*TOC*) content of a source rock from the change in bulk density. In practice this is done by calibrating the log with *TOC* determinations made on core samples from the well or nearby wells, then using the calibrated relationship to calculate *TOC* in the uncored intervals of the well.